Eur. Phys. J. D **33**, 393–398 (2005)
DOI: 10.1140/epjd/e2005-00065-1

THE EUROPEAN PHYSICAL JOURNAL D

Photoionisation using Kohn-Sham wave functions

M. Walter[a] and H. Häkkinen

Department of Physics, Nanoscience Center, University of Jyväskylä, 40014 Jyväskylä, Finland

Received 2nd February 2005 / Received in final form 10 March 2005
Published online 3 May 2005 –

Abstract. The determination of photoionisation cross-sections using the Kohn-Sham wave functions from accurate density functional theory (DFT) calculations is considered. The continuum electrons wave function is specified by its momentum measurable in the detector rather than fixed angular momentum and energy. The method is applied to the test case of a water molecule, where the DFT calculations show excellent agreement to experiment in the ionisation energies if a vertical transition is considered. The continuum electron is described by an analytical wave function and the matrix elements are calculated in both in length and velocity form of the dipole operator. The cross-sections agree well with the experiment in particular for the velocity form.

PACS. 31.15.Ew Density-functional theory – 33.80.Eh Autoionization, photoionization, and photodetachment

1 Introduction

The process of photoionisation or photodetachment and the subsequent measurement of the emitted electron is a useful and direct tool to determine the electronic structure of a system under study. Measuring energy dependent cross-sections and asymmetry parameters does not only involve binding energies [1], but is sensitive to the form of electronic wave functions [2]. Considering larger atoms, molecules or clusters, it is impossible to calculate the many electron wave function directly. Effective one-particle methods like Hartree-Fock or Kohn-Sham density functional theory (DFT) [3] can be used and are standard tools to study the electronic structure of extended systems. It has been shown, that the photoionisation process can be described on the basis of these calculations [4–7] and that even relaxation effects of the whole electron cloud can be described using the linear response of the so-called time dependent DFT [8–10].

Starting from the description of atoms the current theory is formulated in angular momentum expansions of the wave functions involved. However, many ground state calculations of extended systems are done on grids in momentum and/or configuration space leading to accurate results for excitation energies [11]. The construction of the continuum state (needed in the ionisation process) has not been studied in these approaches. One can think of representing the continuum state in a one center angular momentum basis where sophisticated methods exist to find the continuum solution of the Schrödinger equation [12–14]. However, the one centre expansion gets less adequate with increasing system size, involving many angular momentum components which make this expansion cumbersome. In addition, the mapping on the grid of the initial state would perhaps produce uncontrollable errors through the different methods of discretisation used.

In the current work, we propose a different approach to the process than the usual view of continuum states of fixed energy and angular momentum. We view the continuum states in a more experimental way, i.e. the electron in the final state has a definite momentum measurable at the detector, rather than fixed energy and angular momentum. The specification of a defined direction involves all angular momenta and the main purpose of this work is to show how the determination of photoionisation cross-sections can be done in this formalism.

The paper is organised as follows. In Section 2 the formulation of the theory to describe photoinisation is given. Section 3 shows the results of the calculation for the test case of photoionisation of the water molecule. The conclusions are given in Section 4.

2 Theory

We are considering the general photoionisation or photodetachment process of some system with charge $Z-1$ (-1 from the additional electron) absorbing a photon γ of energy ω and emitting one electron. This electron can be measured with momentum $\mathbf{k}$ in the detector, so that the process is schematically

$$\mathsf{S}^{Z-1} + \gamma(\omega) \rightarrow \mathsf{S}^{Z} + e^{-}(\mathbf{k}).$$

[a] e-mail: michael.walter@phys.jyu.fi

The perturbation theory cross-section for this process is given by [15]

$$\frac{d\sigma(\omega)}{d\mathbf{k}} = \frac{(2\pi)^2}{c}\,\frac{1}{\omega}\,|T_{fi}|^2\;\;\delta(E_i+\omega-E_f), \qquad (1)$$

where c is the speed of light and T_{fi} denotes the transition matrix element. The energy E_i is the energy of the initial state and E_f is the energy of the system plus electron in the final state. Atomic units are used throughout unless otherwise specified. Note, that we have written the cross-section (1) differential in $\mathbf{k}$ rather than in the electron energy and emission angle. This is because we will later on describe the continuum state of the electron for a definite direction $\mathbf{k}$ to be measured in the detector.

Experimental photoionisation data is usually recorded for unknown relation between the laboratory frame, in which the vectors $\hat{\boldsymbol{\epsilon}}$ (polarisation) and $\mathbf{k}$ are defined, and the body fixed frame of the system in which the electronic initial state wavefunctions are defined. To compare with experimental data, we therefore have to average over all relative orientations of these frames. Dipole symmetry implies that the averaged cross-section $\bar{\sigma}$ may be expressed in the well-known form [2,16]

$$\frac{d\bar{\sigma}(\omega)}{dE d\hat{\mathbf{k}}} = k\frac{d\bar{\sigma}(\omega)}{d\mathbf{k}} = \frac{1}{4\pi}\,\frac{d\bar{\sigma}(\omega)}{dE}\left(1+\beta(\omega)\,P_2(\hat{\boldsymbol{\epsilon}}\cdot\hat{\mathbf{k}})\right) \qquad (2)$$

where $E = k^2/2$ denotes the electrons kinetic energy at the detector. The parameter β is the asymmetry parameter and $P_2(x) = (3x^2-1)/2$ is the Legendre polynomial of degree 2. Therefore the averaged cross-section just depends on two parameters for fixed photon energy. This is not valid if the systems orientation is fixed in the experiment, where the only valid form of the cross-section is given by equation (1). The two parameters are fixed if the cross-section (2) is known at two relative angles between $\hat{\boldsymbol{\epsilon}}$ and $\hat{\mathbf{k}}$. A useful choice is $\cos\theta_0 = \hat{\boldsymbol{\epsilon}}\cdot\hat{\mathbf{k}} = 1$ and the so-called "magic angle", where $\cos\theta_m = \hat{\boldsymbol{\epsilon}}\cdot\hat{\mathbf{k}} = 1/\sqrt{3}$. At the latter angle $P_2(\cos\theta_m) = 0$ and the cross-section is proportional to the angle integrated cross-section. We therefore specify two situations where $\mathbf{k}$ and $\hat{\boldsymbol{\epsilon}}$ are fixed relative to each other and use the form (1) to evaluate the averaged cross-sections there. If we denote the two cross-sections by $\bar{\sigma}_0, \bar{\sigma}_m$ (for θ_0 and θ_m respectively) we are able to reconstruct the parameters of (2) to be

$$\frac{d\bar{\sigma}}{dE} = \frac{\bar{\sigma}_m}{4\pi}, \quad \beta = \frac{\bar{\sigma}_0}{\bar{\sigma}_m} - 1 \qquad (3)$$

where all parameters still depend on the photon energy.

To simplify the description we view the system in a single particle picture, where the electrons occupy effective mean field states $|\,i\,\rangle$. The states are eigenstates of an effective single particle Hamiltonian $\hat{h}$ with energy e_i. In practice, the eigenstates are Kohn-Sham orbitals from a Born-Oppenheimer (BO) DFT calculation (for the method, see Ref. [17]). Exchange and correlation were treated within local-spin-density (LSD) approximation and generalised gradient corrections (GGA) [18] have been self-consistently applied. The nuclei are relaxed to the energy minimum of the BO surface.

There is no rigorous proof, that the Kohn-Sham orbitals have a meaning other than being a mathematical construct, but it is a well-known experience, that the orbitals can be treated as existing in ionisation processes [3,19,20]. However, the GGA orbital energies e_i are incorrect when compared to exact calculations, but this can be cured approximately by shifting them by a constant [21–23]. This constant can be determined by using the condition, that the negative of the eigenenergy of the highest occupied orbital (HOMO) equals the ionisation potential. This equality is fulfilled in an exact Kohn-Sham formalism [24]. We calculate the ionisation potential I as the difference between the total energy of the system before ionisation $E(\mathsf{S}^{Z-1})$ and the total energy of the system after ionisation $E(\mathsf{S}^{Z})$ at the same nuclear configuration. Assuming that the nuclei do not move during the photoionisation process, the configuration to use is the BO potential minimum of the initial system S^{Z-1}. The corrected orbital energies ε_i are then given by

$$\varepsilon_i = e_i - [e_0 + I] \qquad (4)$$

where the HOMO has the index 0.

We describe the photoionisation process entirely in the single particle picture. In this picture, the electron in the initial state $|\,i\,\rangle$ completely absorbs the photon's energy and is emitted to the continuum state $|\,f\,\rangle$ directly. The matrix element T_{fi} for absorbing a photon of polarisation $\hat{\boldsymbol{\epsilon}}$ in dipole approximation is given in the so-called velocity form by

$$T^V_{fi} = \langle\, i\,|\,\hat{\boldsymbol{\epsilon}}\cdot\nabla\,|\,f\,\rangle \qquad (5)$$

and in the so-called length form by

$$T^L_{fi} = (\varepsilon_i - \varepsilon_f)\,\langle\, i\,|\,\hat{\boldsymbol{\epsilon}}\cdot\mathbf{r}\,|\,f\,\rangle \qquad (6)$$

where $\mathbf{r}$ and ∇ denote the electron's position and it's derivative respectively. The two forms are equivalent if $|\,i\,\rangle$ and $|\,f\,\rangle$ are eigenstates of the same Hamiltonian and non-local effects are negligible [25]. Note, that we have to use the corrected energy ε_i in (6) as it defines the relative energy difference to the free electron (ε_f). In case we would use e_i instead of ε_i, we would get a wrong energy difference to $\varepsilon_f = k^2/2$, which is the true energy measurable in the detector and *not* the unshifted energy of the continuum state in the LSD-GGA potential.

The only part missing at this stage of our description is the final state of an electron in the continuum of the system S^Z that can be measured with momentum $\mathbf{k}$ in the detector. To our knowledge, this problem has not yet been treated for arbitrary potentials. Therefore we apply a simplified model where we assume that the charge Z is concentrated in the centre of mass of the molecule. Then we have a hydrogen like continuum, for which the continuum state is well-known and given by [26,27]

$$\langle\,\mathbf{r}\,|\,\mathbf{k}\,\rangle = N(\alpha)\,\frac{e^{i\mathbf{k}\cdot\mathbf{r}}}{(2\pi)^{3/2}}\;{}_1F_1(i\alpha,1,-i[\mathbf{k}\cdot\mathbf{r}+kr]) \qquad (7)$$

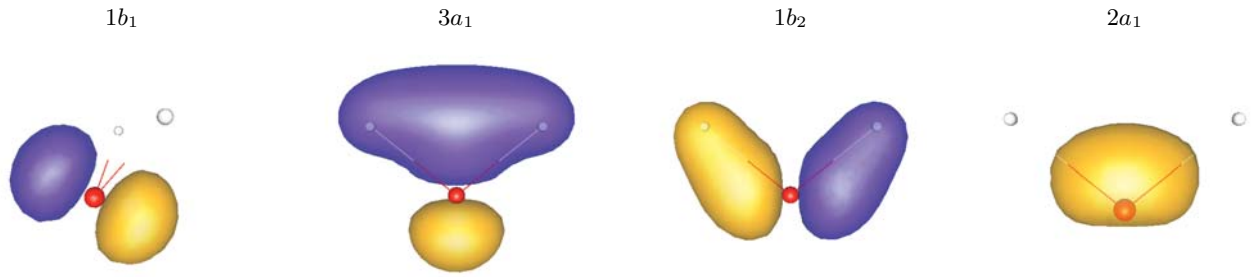

Fig. 1. Visualisation of the molecular orbitals as result of DFT calculations. $1b_1$ is the HOMO state. Dark and light spheres denote O and H atoms, respectively. The $1b_1$ orbital is rotated out of the plane of the paper in order to show its "lone pair" character (essentially an oxygen p-orbital perpendicular to the HOH plane).

where ${}_1F_1$ denotes the confluent hyper-geometric function [28] and the parameter $\alpha = -Z/k$ represents the strength of Coulomb force. The normalisation is given by

$$N(\alpha) = e^{-\pi\alpha/2}\,\Gamma(1 - i\alpha) \tag{8}$$

where Γ denotes the Gamma function [28]. The wave function is normalized to delta function in momentum space and it represents simultaneously an incident wave and an incoming scattered wave as indicated for a scattering final state [29]. The wave function (7) is commonly used in the description of atomic scattering processes and can be generalised easily to describe continua of more than one electron [30].

As was said above, the equality of velocity and length form matrix elements is given only if the initial and final states are eigenstates of the same Hamiltonian. This is not the case anymore if we use numerical orbitals $|\,i\,\rangle$ which are eigenstates of the effective Kohn-Sham Hamiltonian, but the wave function (7) is an eigenstate of a hydrogen like Hamiltonian. Therefore we can expect differences between the cross-sections using the two forms of the dipole operator and their amount gives a criterion on how accurate our simple picture of the continuum is.

3 Results

We apply our description to the test case of water, where extensive experimental data is available. The water molecule has 10 electrons, where two of them are bound in the $1s^2$ core of the oxygen atom and are not explicitly treated here. The other 8 electrons can be viewed as occupying the deformed $2s$ and $2p$ orbitals of the oxygen atom, creating molecular orbitals. These orbitals are labeled due to their molecular symmetry in the order of increasing binding energy as $1b_1$, $3a_1$, $1b_2$ and $2a_1$ [31].

The DFT ground state calculation was done on a uniform plane wave grid with grid spacing 0.22 a_0 corresponding to a plane wave cutoff of 204 Ry. The box contained 80 points in each direction [32]. The $2s^2$ and $2p^4$ valence electrons of oxygen were treated with norm conserving non-local pseudopotentials [33] with core radii of 1.45 a_0. The hydrogen s electron and the proton were treated with a non-divergent local potential with a core radius of 0.95 a_0. Relaxation of the nuclei to their BO energy minimum leads to a HOH angle of 104.4°, which is in excellent agreement with the experimental value of 104.5° [34]. The OH bond length of 0.972 Å is slightly too large compared to the experimental value of 0.958 Å [34].

Table 1. Orbital uncorrected (e_i) and corrected energies (ε_i) compared with experimental ionisation potentials taken from [19]. All quantities are in eV.

orbital	$-e_i$	$-\varepsilon_i$	experiment
$1b_1$	7.19	12.6	12.62
$3a_1$	9.27	14.69	14.74
$1b_2$	13.04	18.46	18.55
$2a_1$	25.1	30.5	32.2

Figure 1 shows images of the Kohn-Sham orbitals in our calculations. The wave functions correspond excellently to the expected symmetries of the molecular orbitals [31]. The uncorrected and corrected orbital energies from our calculation are compared to experimental values in Table 1. The corrected values (applying a shift of 5.41 eV) agree very well with the experimental ionisation potentials, except for the $2a_1$ which differs by about 1.7 eV. Note, that the agreement is at the same level as the agreement achieved by the use of exchange-correlation potentials constructed by statistical averaging in reference [19], which also documented the difficulty of getting correct energies for the $2a_1$ state. Here we note, that we get the same ionisation potential for the HOMO state (12.6 eV) also by using the transition state approximation [3] (that is solving for the eigenvalue of the half-occupied HOMO).

The Kohn-Sham orbitals found can now be used to calculate the photoionisation cross-sections and β parameters for each of the states. The averaging over all possible orientations of the molecular frame is done by averaging over all possible Euler angles ϕ, θ, ψ used to rotate the vectors $\mathbf{k}$ and $\hat{\boldsymbol{\epsilon}}$ to this frame. Here Gauss quadrature using 8 points in each angle is tested to be sufficient to reach convergence.

Figure 2 shows the comparison of the state resolved cross-sections to experimental data taken from references [35,36]. One notes a good quantitative agreement

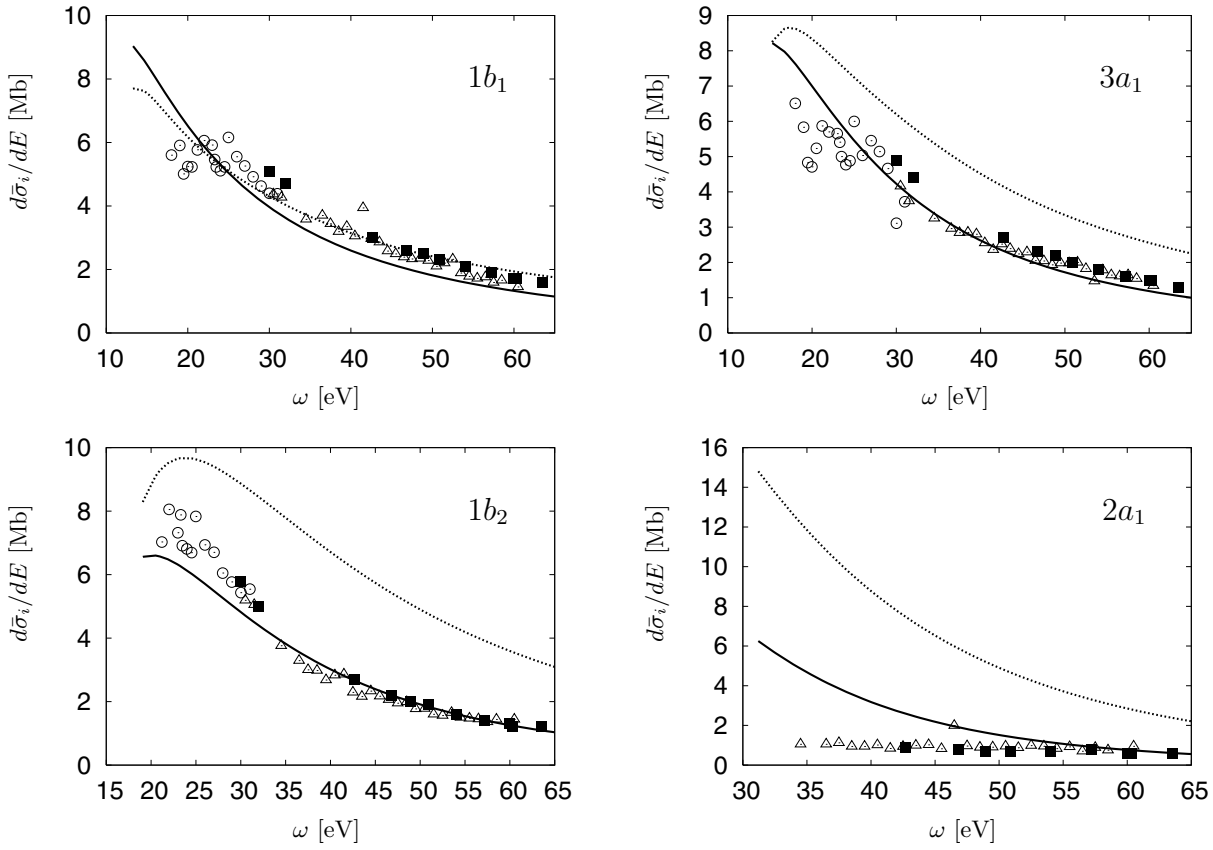

Fig. 2. The state resolved cross-sections in velocity form (full line) and in length form (dotted line) compared to the experiment. The data is taken from [35] (black boxes), Tan et al. as given in [35] (open triangles) and [36] (open circles).

between the velocity form calculations and the experiment for the outer valence orbitals $1b_1$, $3a_1$ and $1b_2$, with a large deviation for the inner valence orbital $2a_1$. The length form cross-section however, agrees with experimental data for the $1b_1$ state only.

The agreement for the $1b_1$ can be understood, if one notes, that this is a lone pair orbital which essentially represents an almost unperturbed p-orbital of the oxygen atom as can be seen in Figure 1. Hence our atomic description of the final state is adequate in this case, as is confirmed by the simultaneous agreement between velocity form, length form and experiment. The good agreement between the velocity form cross-sections with experimental values of the other two valence orbitals $3a_1$ and $1b_2$ can correspond to the favour of the velocity form for higher transition energy [37].

The agreement with the experiment breaks down in the description of the $2a_1$ cross-section, as was indicated already by the difficulty in getting the correct ionisation potential. However, one has to note, that the theoretical curves shown are purely ab initio and not corrected to experimental ionisation potentials like in other calculations [10]. Any error in the ionisation potential enters both in the purely geometrical density of continuum states as well as in the connection of the different dipole transition matrix elements (5) and (6). Therefore a shift of the ionisation potential to the experimental value would improve the agreement with experiment.

Figure 3 shows the experimental β parameters compared to the calculations. Here the agreement between theory and experiment is not as good as in the case of the cross-sections: only the velocity form result for the $1b_1$ orbital is in quantitative agreement with the experiment. The qualitative trend of the β parameter, which rises as the energy increases, is described, but the value is too large nearly everywhere. The reason for this deviation can be attributed to the fact, that the β parameters involve relative phases between the different channels to the continuum and are therefore much more sensitive to even small perturbations of the potentials involved [2].

Our β parameter calculations for the $2a_1$ state show basically $\beta = 2$ as is expected for an s state when no final state interaction is considered. The spherically symmetric potential considered in the construction of the final state (7) is unable to change the angular momentum of the continuum electron. The only source of deviations from $\beta = 2$ in our description is the displacement of the oxygen atom from the molecular centre of mass and the mixing of higher angular momenta into the deformed initial s-state wave function. Both effects are seen to be small and therefore we address the strong deviation from $\beta = 2$ seen in the experiment to be mainly a final state effect.

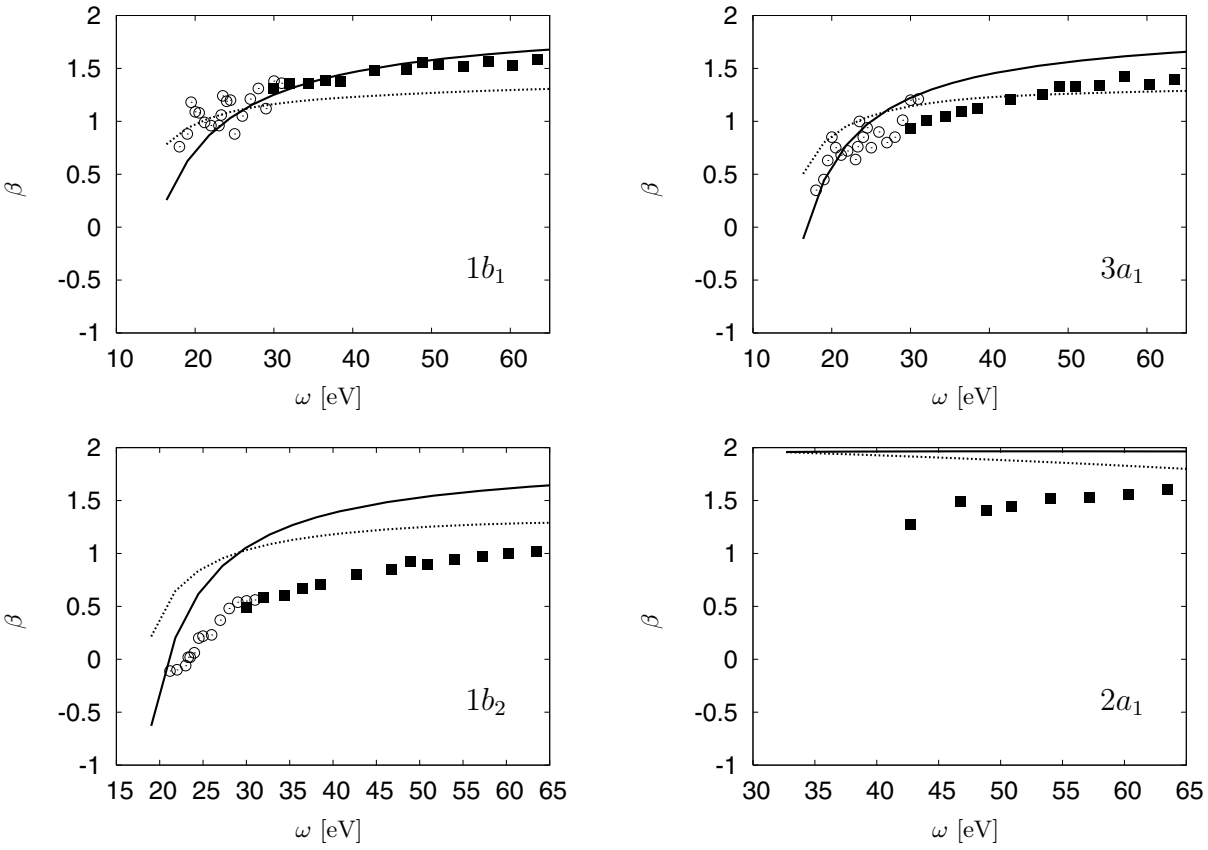

Fig. 3. The state resolved beta parameters in velocity form (full line) and in length form (dotted line) compared to the experiment. The data is taken from [35] (black boxes) and [36] (open circles).

4 Conclusions

We have discussed an approach to describe the photoionisation cross-sections and β parameters which is an alternative to the usual angular momentum expansion description. The ionisation cross-section was formulated differential in the direction of the electron momentum and it is shown how this description can be used to determine photoionisation cross-sections and asymmetry parameters.

The description is applied to the test case of gas phase water molecules, where the initial states are determined by DFT LSD-GGA calculations. These calculations give orbital ionisation energies in very good agreement with the experiment if the binding energy of the HOMO is forced to agree with the negative of the ionisation potential. This procedure provides ionisation energies with errors less than 0.1 eV for the outer valence orbitals.

The difficulty remains in constructing a final continuum state appropriate to the Kohn-Sham potential and describing an electron measurable with a defined momentum in the detector. To circumvent this problem, the final state was described by a hydrogen like continuum wave function, where the wave function is known analytically. This simple approach can describe the cross-sections of the valence orbitals reasonably. However, the description of the more sensitive asymmetry parameter is concordant with experiment for the atom-like $1b_1$ orbital of water only.

The authors acknowledge funding from the Academy of Finland (project 7103219). The BO DFT calculations where performed at the CSC — the Finnish IT Center for Science in Espoo.

References

1. J.C. Green, P. Declava, Coord. Chem. Rev. **249**, 209 (2005)
2. S.T. Manson, *Many-Body atomic physics* (University Press, Cambridge, 1998), chapter 7
3. R.G. Parr, W. Yang, *Density-Functional Theory of Atoms and Molecules* (Oxford Science Publications, Oxford University Press, New York, 1989)
4. I. Wilhelmy, L. Ackermann, A. Gorling, N. Rosch, J. Chem. Phys. **100**, 2808 (1994)
5. R. Díez Muino, D. Rolles, F.J. García de Abajo, C.S. Fadley, M.A. Van Hove, J. Phys. B **35**, L359 (2002)
6. A.P.P. Natalense, L.M. Brescansin, R.R. Lucchese, Phys. Rev. A **68**, 032701 (2003)
7. D. Toffoli, M.J. Simpson, R.R. Lucchese, Phys. Rev. A **69**, 062712 (2004)
8. A. Zangwill, P. Soven, Phys. Rev. A **21**, 1561 (1980)
9. M. Stener, P. Decleva, A. Lisini, J. Phys. B **28**, 4973 (1995)

10. M. Stener, G. Fronzoni, D. Toffoli, P. Decleva, Chem. Phys. **282**, 337 (2002)
11. M. Moseler, H. Häkkinen, U. Landman, Phys. Rev. Lett. **87**, 053401 (2001)
12. R.R. Lucchese, V. McKoy, Phys. Rev. A **21**, 112 (1980)
13. S. Nagano, S.Y. Tong, Phys. Rev. B **32**, 6562 (1985)
14. M. Brosolo, P. Decleva, Chem. Phys. **159**, 185 (1992)
15. R.R. Lucchese, V. McKoy, Phys. Rev. A **26**, 1992 (1982)
16. R.N. Zare, *Angular Momentum* (John Wiley & Sons, 1988)
17. R.N. Barnett, U. Landman, Phys. Rev. B **48**, 2081 (1993)
18. J.P. Perdew, K. Burke, M. Ernzerhof, Phys. Rev. Lett. **77**, 3865 (1996)
19. D.P. Chong, O.V. Gritsenko, E.J. Baerends, J. Chem. Phys. **116**, 1760 (2002)
20. M. Moseler, B. Huber, H. Häkkinen, U. Landman, G. Wrigge, M. Astruc Hoffmann, B.V. Issendorff, Phys. Rev. B **68**, 165413 (2003)
21. D.J. Tozer, N.C. Handy, J. Chem. Phys. **108**, 2545 (1998)
22. J. Akola, M. Manninen, H. Häkkinen, U. Landman, X. Li, L.-S. Wang, Phys. Rev. B **60**, R11297 (1999)
23. A. Wasserman, N.T. Maitra, K. Burke, Phys. Rev. Lett. **91**, 263001 (2003)
24. C.-O. Almbladh, U. von Barth, Phys. Rev. B **31**, 3231 (1985)
25. A.F. Starace, Phys. Rev. A **3**, 1242 (1971)
26. M.R.C. McDowell, J.P. Coleman, *Introduction to the theory of ion-atom collisions* (North-Holland publishing company, Amsterdam-London, 1970)
27. H. Klar, Z. Phys. D **16**, 231 (1990)
28. *Handbook of Mathematical Functions*, edited by M. Abramovitz, I.A. Stegun (Dover Publications, Inc., New York, 1972)
29. G. Breit, H.A. Bethe, Phys. Rev. **93**, 888 (1954)
30. M. Brauner, J.S. Briggs, H. Klar, J. Phys. B **22**, 2265 (1989)
31. P.W. Atkins, *Molecular quantum mechanics* (Oxford university press, 1970)
32. These values were carefully checked to be converged both in the resulting structure and in the orbital energies
33. N. Troullier, J.L. Martins, Phys. Rev. B **43**, 1993 (1991)
34. *CRC Handbook of Chemistry and Physics*, edited by R.C. Weast, 66th edn. (CRC Press, Inc. Boca Raton, Florida, 1985)
35. M.S. Banna, B.H. McQuaide, R. Malutzki, V. Schmidt, J. Chem. Phys. **84**, 4739 (1986)
36. C.M. Truesdale, S. Southworth, P.H. Kobrin, D.W. Lindle, G. Thornton, D.A. Shirley, J. Chem. Phys. **76**, 860 (1982)
37. M.T. Anderson, F. Weinhold, Phys. Rev. A **10**, 1457 (1974)